JOURNAL OF MATERIALS SCIENCE 26 (1991) 11–16

Dislocation configurations in high T_c oxide BiSrCaCuO

C. SONG
TEM Laboratory, Department of Alloy Steels, Central Iron and Steel Research Institute, Beijing 100081, People's Republic of China

F. LIU‡, H. GU‡, T. LIN‡, J. ZHANG, G. XIONG, D. YIN*
Department of Physics, Peking University, Beijing 100871, People's Republic of China,
**and also, Center of Condensed Matter and Radiation CCAST (World Laboratory)*

A study of dislocation configurations in superconducting oxide BiSrCaCuO has been made by transmission electron microscopy. Evidence was found for the presence of dislocation pairs composed of two parallel single dislocations holding together with the same Burgers vectors. The pair can further dissociate into partials, giving rise to a four-fold ribbon. Networks consisting of dislocation pairs were also observed. These phenomena are attributed to the possible ordering of strontium and calcium ions and the existence of some oxygen sheet of the Aurivillius type in the oxide crystal. Schemes to illustrate the configurations are suggested and discussed.

1. Introduction

The discovery of high T_c BiSrCaCu oxide [1] has generated an enormous amount of activity in study on this new system. While many different models for the lattice structure [2–4] as well as for the modulation in these compounds [5, 6] have appeared, there are still few reported results on the dislocation arrangements, though the latter are also important for understanding the real behaviour of these materials.

The present work was devoted to an experimental study of dislocations in BiSrCaCu oxide. By the use of transmission electron microscopy (TEM) with diffraction contrast, various dislocation configurations in thin-foil specimens have been observed in detail. In order to identify dislocations of different types, the determination of Burgers vectors is primarily emphasized. Possible schemes to illustrate the configurations are discussed. For the purpose of insuring the proper contrast effects, a brief analysis of the relative intensity distribution of the main selected-area diffraction pattern (SAD) is introduced at the beginning of this paper.

2. Experimental procedure

TEM specimens were thin foils prepared by magnetron sputtering on (1 0 0) $SrTiO_3$ substrate. Raw materials for fabricating the targets were mixed and sintered oxide powders with the metal-ion stoichiometry as $Bi_4Sr_4Ca_2Cu_4$. Under plastic protection, the films were removed from the substrate. Owing to repeated cleavage, the samples finally obtained often qualified for TEM observations. The preliminary lattice parameters of the films were proved by X-ray diffraction data to be $a = b = 0.38$ nm, $c = 3.07$ nm with a tetragonal unit cell. By standard four-probe resistivity measurement the zero-resistance temperature was determined as 77 K and onset T_c above 100 K. TEM observations were carried out using a 200 kV (H-800) analytical electron microscope equipped with a double tilt holder.

3. Results

3.1. A brief approach to the distribution of diffraction intensities from the reflections of the [0 0 1] zone

In most cases the surface of the thin films obtained by magnetron sputtering were parallel to the (0 0 1) crystallographic plane, i.e. the close-packed plane along which slip and cleavage can easily occur. In order to observe dislocations on this plane under a succession of two-beam conditions, a good understanding of the diffraction intensity distribution of the [0 0 1] SAD pattern is necessary. A simple way to achieve this is to calculate the structure factors of the [0 0 1] zone and then compare them with a real diffraction pattern.

The basic expression for calculating the structure factor F_{hkl} is

$$F_{hkl} = \sum_i f_i(\theta)\exp - [2\Pi i(hX_i + kY_i + lZ_i)] \quad (1)$$

X_i, Y_i, Z_i are the structure parameters (atomic coordinates). The data chosen were in accordance with the model of atomic arrangement of BiSrCaCu oxide suggested by Tang *et al.* [4] (see Table I). Thus we

‡ Graduate student

0022–2461/91 $03.00 + .12

TABLE I Structure parameters of $Bi_4Sr_4Ca_2Cu_4O_{20-\delta}$ [4]: atomic fractional coordinates

Atom	x	y	z
Bi(1)	0.5000	0.5000	0.2009(2)
Bi(2)	0.0000	0.0000	0.3030(3)
Cu(1)	0.5000	0.5000	0.0629(2)
Cu(2)	0.0000	0.0000	0.4438(5)
X_1	0.0000	0.0000	0.0000
Sr	0.0000	0.0000	0.1209(6)
X_2	0.5000	0.5000	0.3910(6)
Ca	0.5000	0.5000	0.5000
O(1)	0.0000	0.5000	0.0563(8)
O(2)	0.5000	0.0000	0.0563(8)
O(3)	0.5000	0.5000	0.1336(9)
O(4)	0.0000	0.0000	0.2010(10)
O(5)	0.0000	0.5000	0.2525(10)
O(6)	0.5000	0.0000	0.2520(10)
O(7)	0.5000	0.5000	0.3030(10)
O(8)	0.0000	0.0000	0.3709(15)
O(9)	0.5000	0.0000	0.4485(5)
O(10)	0.0000	0.5000	0.4485(5)

Note: X_1(0.5 Sr, 0.5 Ca), X_2(0.75 Sr, 0.25 Ca).

have

$$F_{hk0} = 4f_{Bi} + 4f_{Sr} + 2f_{Ca} + 4f_{Cu} + 18f_0$$
when $l=0$, h,k are all even (2)

$$F_{hk0} = 4f_{Bi} + 4f_{Sr} + 2f_{Ca} + 4f_{Cu} - 1.8f_0$$
when $l=0$, h,k are all odd (3)

$$F_{hk0} = f_{Sr} - f_{Ca}$$
when $l=0$, h,k are mixed even and odd (4)

After introducing the values of atomic scattering amplitude $f(\theta)$ [7] into the expressions, the data in Table II are obtained. It can be seen when h,k are mixed even and odd, such as 100, 300, 120, etc., the structure factor values are very small, near vanishing.

Fig. 1 shows the intensity distribution of a real SAD pattern taken with the incident beam parallel to the [001] crystallographic direction of the thin-foil sample. The relative intensities of the main reflections are in agreement with the calculations mentioned above.

With the above results and the estimated gliding directions on (001) planes, the products of $\boldsymbol{g}$ (operating vector for TEM observation under two-beam conditions) and $\boldsymbol{b}$ (possible Burgers vector of dislocations) are calculated as shown in Table III.

3.2. Observation of dislocations

A number of single perfect dislocations have been seen in (001) thin foils. These dislocations are rather long and rather regular in shape. A typical area is exhibited

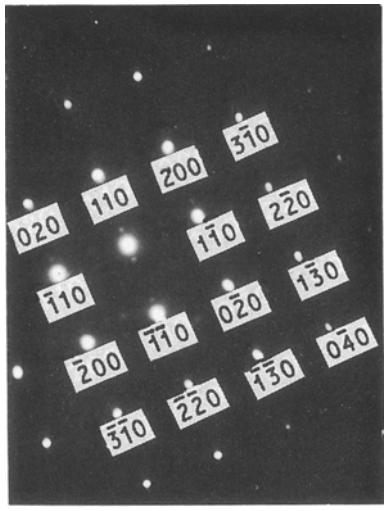

Figure 1 SAD pattern from the [001] zone axis.

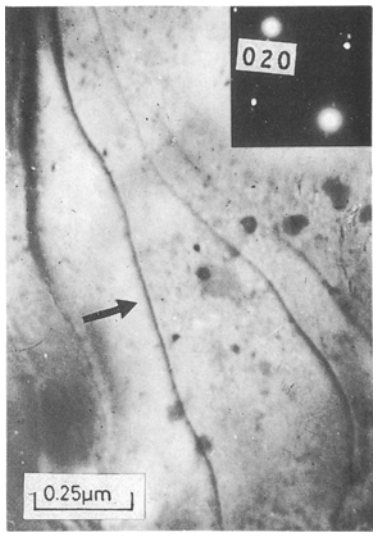

Figure 2 Transmission electron micrograph of the perfect dislocations in BiSrCaCuO.

in Fig. 2. The appearance proves that these dislocations are travelling parallel to the plane surface (001) which functions as the slip plane. A series of two-beam diffraction tests has been performed. With the aid of the $\boldsymbol{g}\cdot\boldsymbol{b}$ invisible criterion [7] and the product values in Table III the Burgers vector is identified as $b = a$ [110].

Fig. 3 shows an interesting example of dislocation networks. Plenty of dislocations are present in the form of a network. In this way dislocations connect with each other in a more stable ensemble. In Fig. 3a to d the operative reflections are sequentially taken as (020), (200), (1 $\bar{1}$ 0), (110). As a consequence, different dislocation families denoted by A, B, C, D in turn lose

TABLE II Structure factors for reflections from the [001] zone

hkl										
100	200	300	400	500	110 $1\bar{1}0$	220 $2\bar{2}0$	330 $3\bar{3}0$	120 $1\bar{2}0$	130 $1\bar{3}0$	230 $2\bar{3}0$
F_{hkl}										
2.3	80.8	1.0	35.9	0.6	76.9	55.7	24.0	1.3	34.7	0.7

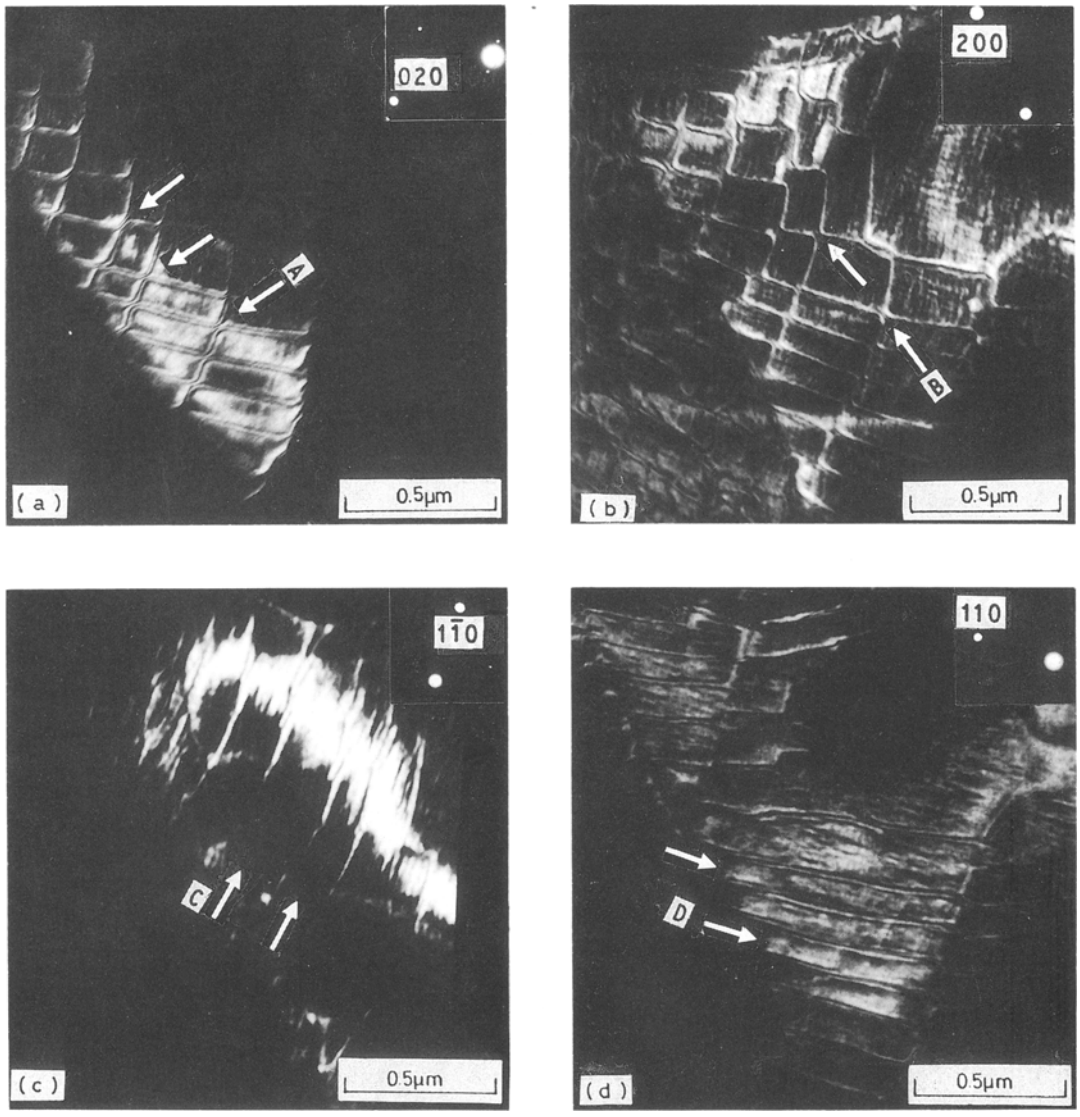

Figure 3 TEM dark-field images showing the dislocation network in BiSrCaCuO. (a) Dislocation array A is invisible, (b) array B is invisible, (c) array C is invisible, (d) array D is invisible.

their contrast. The Burgers vectors are thus determined, respectively, to be $a[1\,0\,0]$, $a[0\,1\,0]$, $a[1\,1\,0]$ and $a[1\,\bar{1}\,0]$. Evidently, this network is arranged in a planar manner parallel to the main slip plane. The basal dislocation arrays C and D with the Burgers vectors $a[1\,1\,0]$ and $a[1\,\bar{1}\,0]$, respectively, are of pure screw character. At the nodes the reactions occur as the following types

$$a[1\,0\,0] + a[0\,1\,0] = a[1\,1\,0] \quad (5)$$

$$a[1\,0\,0] + a[0\,\bar{1}\,0] = a[1\,\bar{1}\,0] \quad (6)$$

Moreover, a notable feature of the fine structure is the frequent occurrence of dislocation pairs. This is, for instance, the case in Fig. 4. Nearby points A and B, the long parallel coupled dislocations display their contrast as the reflecting vector $[1\,1\,0]^*$, see Fig. 4a. When $\boldsymbol{g}$ changes to $[2\,0\,0]^*$, both A and B simultaneously go out of contrast (only very faint residual contrast can be seen), see Fig. 4b. In order to ascertain if the coupled dislocations are a dislocation pair or a dipole, reference was made to the work of Bell *et al.* [8], and the image characteristic was checked by reversing the $\boldsymbol{g}$ operator. The separations between the two parallel dislocations do not change under $\pm[1\,1\,0]^*$. The coupled dislocations are finally identified to be a dislocation pair rather than a dipole. The pair is composed of two single dislocations held together by the same Burgers vectors $a[0\,1\,0]$ (the same values and the same signs). The reaction is

$$a[0\,1\,0] + a[0\,1\,0] = a[0\,2\,0] \quad (7)$$

The total Burgers vector of the pair is $a[2\,0\,0]$. The trace of pairs A and B shows that they are mixed dislocations, mainly with an edge component. Thus some faint residual contrast is left when $\boldsymbol{g} \cdot \boldsymbol{b} = 0$.

The two single dislocations of a pair can be further split into partials. Fig. 5 represents this situation. The

TABLE III Products ($\boldsymbol{g} \cdot \boldsymbol{b}$) for reflections from the [0 0 1] zone

$\boldsymbol{g}$	$\boldsymbol{b}$					
	[0 1 0]	[1 0 0]	1/2[1 1 0]	1/2[1 $\bar{1}$ 0]	[1 1 0]	[1 $\bar{1}$ 0]
[2 0 0]*	0	2	1	1	2	2
[0 2 0]*	2	0	1	−1	2	−2
[1 1 0]*	1	1	1	0	2	0
[1 $\bar{1}$ 0]*	−1	1	0	1	0	2

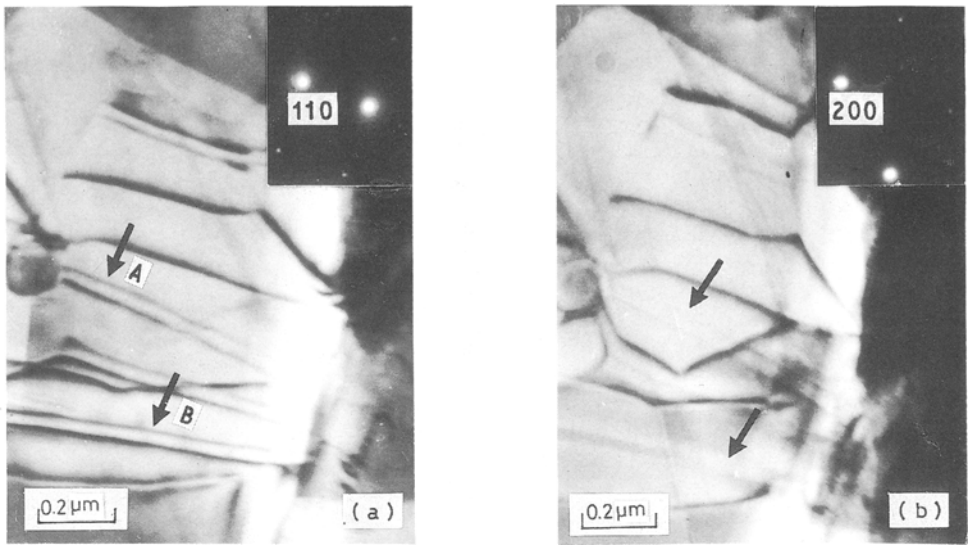

Figure 4 Transmission electron micrographs showing dislocation pairs in BiSrCaCuO. (a) Pairs A and B are visible, (b) A and B are invisible.

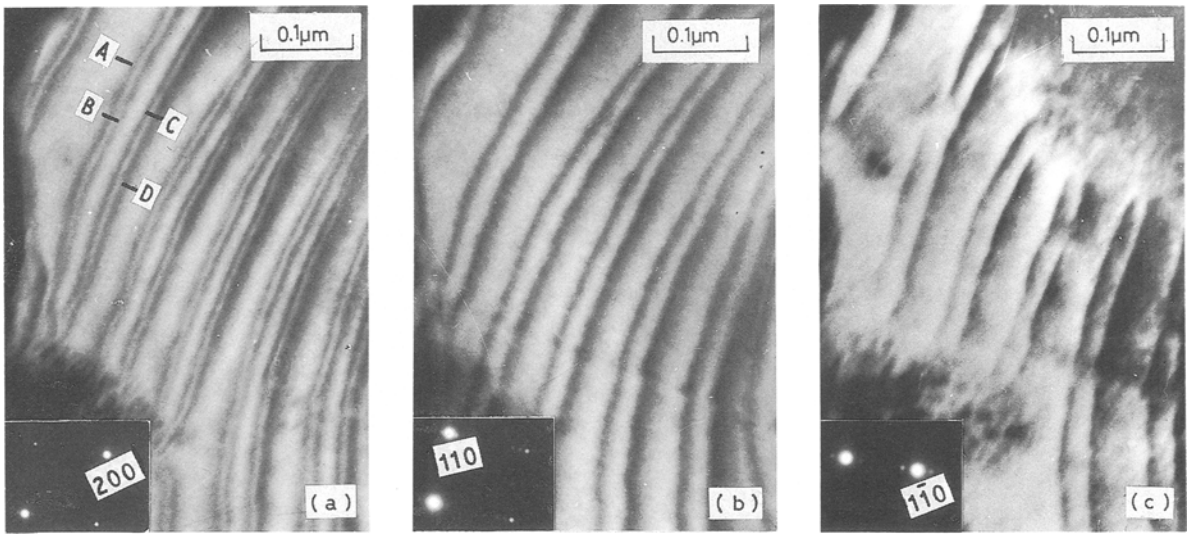

Figure 5 Transmission electron micrographs showing the dissociation of a dislocation pair in BiSrCaCuO. (a) Partials A, B, C, D are all visible, (b) A and C are invisible, (c) B and D are invisible.

dissociation of a dislocation pair gives rise to a four-fold ribbon. In Fig. 5a, $\boldsymbol{g} = [200]^*$, the ribbon is completely visible. The four lines of a ribbon are respectively marked A, B, C and D. In Fig. 5b, $\boldsymbol{g} = [110]^*$, the two partials, A and C, disappear. Conversely, in Fig. 5c, $\boldsymbol{g} = [1\bar{1}0]^*$ another two partials, B and D, are invisible. Apparently, the following reactions occur for this ribbon

$$a[100] + a[100] = a/2[110] + a/2[1\bar{1}0] + a/2[110] + a/2[1\bar{1}0] \quad (8)$$

Because the basal glide plane parallels the foil surface, the projection of the separation between the dissociated partials equals the true perpendicular distance. This value can be easily measured to be about 10 nm. This so widely extended ribbon suggests a low stacking fault energy of the BiSrCaCuO thin foil. More details on this topic have been reported and discussed in another paper [9].

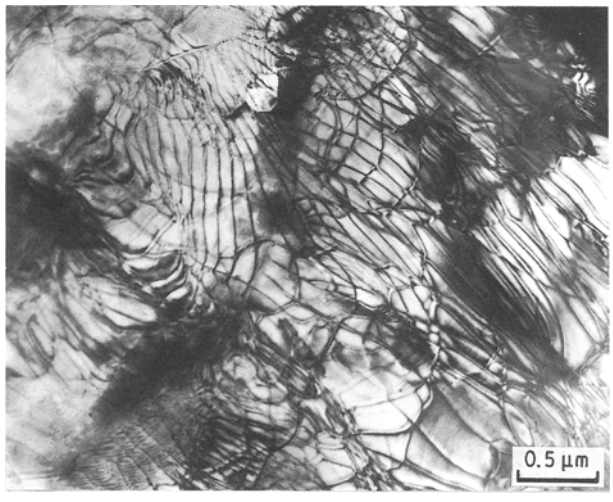

Figure 6 Transmission electron micrograph showing the dislocations densely distributed in BiSrCaCuO.

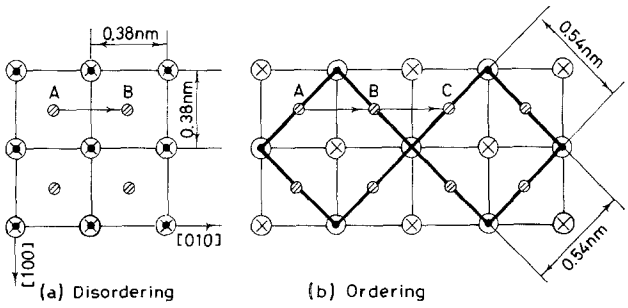

Figure 7 Schematic illustration of the formation of a superlattice dislocation.

Finally, for a statistical survey, the dislocation densities were roughly measured by the method suggested by Hirsch *et al.* [7]. The thickness of the foil was estimated to be ~150 nm. A dislocation pair was taken into account as a total dislocation. As one can imagine, the dislocations always distribute inhomogeneously in a whole specimen. The experimental data for the highest dislocation density is of the order of 10^{10} cm cm^{-2}. Fig. 6 is representative of the dense distribution of dislocations in the present samples. Some networks consisting of dislocation pairs are also often seen.

4. Discussion

It has been seen that at least four kinds of dislocations exist on the (0 0 1) plane with the Burgers vectors of (1) a[0 0 1] (0.38 nm), (2) a[1 1 0] (0.54 nm), (3) a[2 0 0] (0.76 nm), (4) $a/2$[1 1 0] (0.27 nm). The first two types can naturally be expected from the conditions of minimal elastic energy of dislocations, because on the (0 0 1) plane of BiSrCaCuO, atoms are sited as square lattices. However, the dislocation with a large Burgers vector of $\boldsymbol{b} = a$[2 0 0] must be a superlattice dislocation, where the ordered matrix has the lattice period of $2a$. A possible origin of this superlattice is the ordering of strontium and calcium ions in the (Sr 0.5, Ca 0.5) layer (see Table I). A scheme shown in Fig. 7 is thus suggested to illustrate the situation. When the strontium and calcium ions are randomly arranged, the shortest lattice translation vector is a[1 0 0] which is also the shortest Burgers vector of a perfect dislocation (Fig. 7a). However, if ordering is established in this layer, strontium and calcium ions will occupy different sublattices (0.54 nm × 0.54 nm) as shown in Fig. 7b. For an ion in the crystal travelling along the [1 0 0] direction, the environment of A is different from B, but is equivalent to C. In order to restore the original environment a superlattice dislocation forms.

It was also considered whether the ordering arrangement of the (Sr 0.5, Ca 0.5) layer makes any difference to the [0 0 1] SAD pattern. The contributions of the (Sr 0.5, Ca 0.5) layer to the sum structure factor in both ordering and disordering conditions have been calculated. The results are as follows:

(Sr 0.5, Ca 0.5) layer disordering:

$$F_{hk0}(\mathrm{Sr}_{0.5}, \mathrm{Ca}_{0.5}) = \tfrac{1}{2}(f_{\mathrm{Sr}} + f_{\mathrm{Ca}}) \qquad (9)$$

$(\mathrm{Sr}_{0.5}, \mathrm{Ca}_{0.5})$ layer ordering:

$$\begin{aligned} F(\mathrm{Sr}_{0.5}, \mathrm{Ca}_{0.5}) &= \tfrac{1}{4}[f_{\mathrm{Sr}} + f_{\mathrm{Sr}} \cos 2\Pi(h + k) \\ &\quad + f_{\mathrm{Ca}} \cos 2\Pi h + f_{\mathrm{Ca}} \cos 2\Pi k] \\ &= \tfrac{1}{2}(f_{\mathrm{Sr}} + f_{\mathrm{Ca}}) \end{aligned} \qquad (10)$$

Thus the (Sr 0.5, Ca 0.5) ordering has no influence on the intensity distribution of the [0 0 1] SAD pattern.

If ordering occurs in other layers, for instance if some bismuth ions in the Bi–O layer are substituted by other kinds of ions and they are arranged orderly, it may also possibly lead to the formation of a superlattice dislocation. However, it will influence the SAD pattern. In fact, further investigation and direct observation of the atom arrangements in ordering conditions remain to be done by high-resolution electron microscopy.

The Burgers vector $\boldsymbol{b} = a/2$ [1 1 0] represents unambiguously a partial glide dislocation and relates to the shortest lattice translation vector of 0.27 nm. From the suggested structural models so far this kind of translation vector can only be found on some oxygen sheets of the Aurivillius type. Because the shortest vector that connects crystallographically equivalent positions on the oxygen sheet is $a/2$[1 1 0], such a partial glide will not change the bonding configuration between nearest neighboured Bi–O and the oxygen sheet but only alter the configuration between the next-nearest neighboured sheets. Accordingly, the oxide crystal will thus possess a lower stacking fault energy. Recently, a new model for the modulation of BiSrCaCuO has been suggested [10] which supposes that the region with two adjacent rock-salt Bi–O sheets [6] and the region with an Aurivillius oxygen sheet between the bismuth layers, appear alternately with the modulation period as shown in Fig. 8. Because the glide most likely occurs between the bismuth sheets, the evidence of partial $a/2$[1 1 0] dislocation in this compound seems more consistent with this model rather than that of Tarascon *et al.* [6].

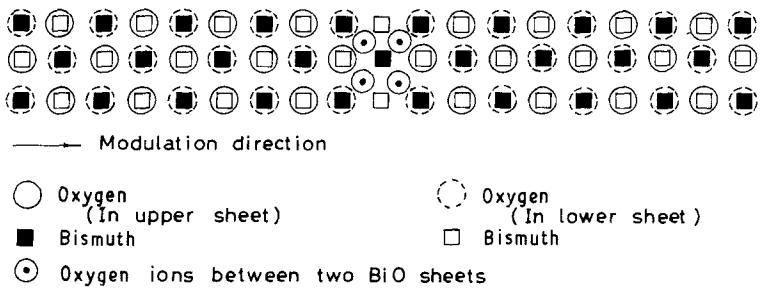

Figure 8 (0 0 1) planar arrangement of oxygen atoms in the modulation model in $Bi_2Sr_2CaCu_2O_{6.21}$ [10].

References

1. H. MAEDA, Y. TANAKA, M. FUKUTOMI and T. ASANO, *Jpn J. Appl. Phys.* **27** (1988) L209.
2. M. A. SUBRAMANIAN, C. C. TORARDI, J. C. CALABRESE, J. GOPALAKRISHNAN, K. J. MORRISSEY, T. R. ASKEW, R. S. FLIPPEN, U. CHOWDHRY and A. W. SLEICHT, *Science* **239** (1988) 1015.
3. J. M. TARASCON, Y. Y. LE PAGE, P. BARBOUX, B. G. BAGLEY, L. H. GREENE, W. R. MCKINNON, G. W. HULL, M. GIROUD and D. M. HWANG, *Phys. Rev. B* **37** (1988) 93829.
4. Y. TANG, B. LIN, X. ZHENG, W. ZHU, Y. ZHANG, Z. LIU and W. ZHANG, *Mod. Phys. Lett.* **B2** (1988) 551.
5. H. W. ZANDBERGEN, W. A. GROEN, F. C. MIJLHOFF, G. VAN TENDELOO and S. AMELINCKX, *Physica* **C156** (1988) 325.
6. J. M. TARASCON, P. F. MICELI, P. BARBOUX, D. M. HWANG, G. W. HULL, M. GIROUD, L. H. GREENE, Y. LE PAGE, W. R. MCKINNON, E. TSELEPIS, G. PLEIZIER, M. EIBSCHUTZ, D. A. NEUMANN and J. J. RHYNE, *Phys. Rev. B* **39** (1989) 11587.
7. P. B. HIRSCH, A. HOWIE, R. B. NICHOLSON, D. W. PASHLEY and M. J. WHELAN, "Electron Microscopy of Thin Crystals" (Butterworths, London, 1971) pp. 263, 422, 489.
8. W. L. BELL, W. R. ROSER and G. THOMAS, *Acta Metall.* **12** (1964) 1247.
9. F. LIU, H. GU, T. LIN, J. ZHANG, G. XIONG, D. YIN and C. SONG, *Mod. Phys. Lett.* **B3** (1989) 1359.
10. D. YIN, X. ZHU and B. LIN, presented at "The Workshop on High T_c Superconducting Materials", Hefei, China, 1–4 April, 1988.

Received 15 August 1989
and accepted 19 February 1990